PALM and STORM : Unlocking Live-Cell Super-Resolution

Ricardo Henriques,[1,2] Caron Griffiths,[3,4] E. Hesper Rego,[5,6] Musa M. Mhlanga[1,3]

[1] Unidade de Biofisica e Expressão Genetica, Instituto de Medicina Molecular, Faculdade de Medicina Universidade de Lisboa, Lisboa, Portugal

[2] Institut Pasteur, Groupe Imagerie et Modelisation, Centre National de la Recherche Scientifique, Unite de Recherche Associe 2582, Paris, France

[3] Gene Expression and Biophysics Group, Synthetic Biology Emerging Research Area, Council for Scientific and Industrial Research, Pretoria, South Africa

[4] Department of Biochemistry, Faculty of Natural and Agricultural Sciences, University of Pretoria, Pretoria, 0002, South Africa

[5] Graduate Group in Biophysics, University of California, San Francisco, CA 94158

[6] Howard Hughes Medical Institute, Janelia Farm Research Center, Ashburn, VA 20147

ABSTRACT:

Live-cell fluorescence light microscopy has emerged as an important tool in the study of cellular biology. The development of fluorescent markers in parallel with super-resolution imaging systems has pushed light microscopy into the realm of molecular visualization at the nanometer scale. Resolutions previously only attained with electron microscopes are now within the grasp of light microscopes. However, until recently, live-cell imaging approaches have eluded super-resolution microscopy, hampering it from reaching its full potential for revealing the dynamic interactions in biology occurring at the single molecule level. Here we examine recent advances in the super-resolution imaging of living cells by reviewing recent breakthroughs in single molecule localization microscopy methods such as PALM and STORM to achieve this important goal.

Keywords: super-resolution; microscopy; single molecule

Correspondence to: Ricardo Henriques; e-mail: rhenriques@fm.ul.pt and Musa M. Mhlanga; e-mail: musa@mhlangalab.org

Ricardo Henriques and Caron Griffiths contributed equally to this work.

INTRODUCTION

Modern cell biology depends extensively on fluorescence light microscopy to provide key insights into cellular structure and molecular behavior. Inherent advantages, such as its non-invasive nature and the ability to use highly specific labeling tools, have made fluorescence light microscopy the preferred strategy for imaging fixed and living cells. The maximum optical resolution of this method is typically restricted to 200-nm laterally and 500-nm axially. This limitation constrains its ability to provide high-resolution structural information on molecules that are central to the dogma of biology, namely DNA, RNA, and protein, which exist as single molecules at scales of few nanometers. The physics-based resolution limit of light microscopes imposed by their optical architecture and the wave nature of light was mathematically described in the 19th century by Abbe.[1]

Electron microscopy (EM) has been able to surpass the resolution limit of optical microscopy and for several years was the routine approach to resolve cellular architecture at the ultra-structural or atomic level. However, EM lacks the basic advantages of fluorescence microscopy such as highly specific multi-color labeling, and live-cell imaging, both of which remain altogether impossible with EM.

In response to this dilemma, recent developments in microscopy have aimed to create techniques able to retain the advantages of fluorescence microscopy while approaching the resolving power of EM. Indeed recent advances in single-molecule localization microscopy (SMLM) have shown resolution below the nanometer.[2] Variants such as photo-activated localization microscopy (PALM),[3] fluorescence PALM (FPALM),[4] stochastic optical reconstruction microscopy (STORM),[5] direct STORM (dSTORM),[6] and PALM with independent running acquisition (PALMIRA)[7–9] have emerged at the forefront of the new ''super-resolution'' methods retaining the labeling advantages of fluorescence imaging. However, these approaches are also hampered by their inability to be robustly used for live-cell imaging.

Ideally to achieve ''EM-like'' resolution while preserving the inherent advantages of live-cell fluorescence microscopy, the imaging needs to be carried out with minimal perturbation of the sample while acquiring multi-wavelength 2D or 3D data rapidly enough to correctly reconstruct a time-lapse movie of the cell behavior, with nanoscopic resolution.[10] Achieving this remains elusive in live-cell SMLM and is currently a major focus in the field necessitating innovations in imaging, microscopy, and sample preparation (termed ''the hardware'') and in computational techniques (termed ''the software'') that permit its routine implementation. For the remainder of this review we will discuss a number of novel strategies to address these goals.

Achieving Single-Molecule Localization

In optical microscopy, any point source of light smaller than the diffraction limit appears with a fixed size and shape represented by an airy disk pattern or otherwise known as the point-spread function (PSF). This spatial broadening effect is dependent on the emission wavelength of the fluorophore and optical characteristics of the imaging apparatus such as the numerical aperture of the objective used. Classically the resolution limit is then calculated by applying Rayleigh's criterion—where the resolution is equal to the minimum distance between observed points that can still be resolved as discrete objects. Since individual elements of molecular assemblies such as DNA, RNA, and proteins exist at scales beyond this limit they cannot be easily distinguished or precisely localized as individual molecules. Thus an important element in achieving single molecule localization is the ''hardware'' challenge.

SMLM represents a suite of approaches able to achieve single molecule detection and localization in fluorescence microscopy. Extremely high nanoscopy resolutions can be achieved either at the sub-nanometer level for few molecules[2] or, more commonly, in the range of tens of nanometers for structural reconstructions involving thousands to millions of fluorescently-labeled objects. Such resolutions are typical of the techniques PALM, FPALM, STORM, dSTORM, and PALMIRA.

Vital to these approaches is the knowledge that the center of the detected emission light from the fluorophores can be localized analytically and computationally with sub-pixel accuracies beyond the classical resolution limit of optical microscopes.[11,12] To make this possible, three important criteria must be satisfied: (a) the number of photons detected for each fluorophore needs to be high enough so as to clearly distinguish individual PSFs from the surrounding background; (b) fluorophore mobility needs to be slow enough, as compared to the image acquisition time, so as to present well-defined PSFs without considerable blur effects from motion; (c) particle PSFs cannot overlap extensively or they will lead to an increase in the complexity of analytical segmentation and localization of neighboring fluorophores.

Meeting these criteria in live-cell imaging has proven to be a difficult challenge. Several factors can negatively influence the ability to satisfy the above criteria. These include motion of cellular and sub-cellular components and light-induced damage caused by laser illumination. The toxicity of aqueous solutions needed to manage the photo-dynamic behavior of fluorophores further hinders live-cell imaging. Finally variable levels of density and detection of the objects due to biological stochasticity complicate the localization of individual molecules. Thus the ''hardware'' challenges for live-cell SMLM span from the optical setup and architecture of the microscope to the sample preparation and buffer conditions under which image

acquisition is achieved.

Super-Resolving Large Populations of Fluorophores

PALM, FPALM, STORM, and dSTORM present a solution for some of these dilemmas by combining the sequential acquisition of images with the stochastic switching-on and -off of fluorophores. By regulating the number of active fluorophores in each time-instance through a light-induced environment it is possible to minimize the probability that in any given image two or more particles spatially overlap, thus satisfying condition (c). A super-resolution dataset can then be reconstructed by plotting the accumulation of the localized particles from a sequence of images. The final resolution of the reconstruction depends only on the localization precision for each fluorophore, which in turn depends upon the particle's observable signal-to-noise ratio. Effectively, several hundred to thousands of images can be collected until enough detected molecules are accumulated to accurately generate a super-resolution dataset where cellular ultra-structure can be highly resolved. The speed of raw-data acquisition is thus dependent on the rate at which sufficient particles can be detected with enough photons to be precisely localized (see Figure 1).

The concept of image and time-point becomes complex when dealing with these methods. Generally a single acquired image does not fully illustrate a time-point as it contains too few detected molecules to resolve a biological structure, such as a cytoskeletal framework, for example. As a solution, multiple images may need to be gathered (typically hundreds) in a sufficiently short time, to represent the state of a structure for the duration of the time-point acquisition while preventing unwanted cell motion artifacts. In these methods, fluorophore mobility has to be slow enough in order to retain the ability to detect and localize moving objects so as not to violate aforementioned condition (b). As a result, published live-cell SMLM experiments to date have only been able to study complexes that are slow in nature. Hess et al. used FPALM to study slow moving membrane proteins in fibroblasts at 40-nm resolution,[13] while Shroff et al. used PALM to study adhesion-complex dynamics using 25–60 s per frame, at 60-nm resolution.[14]

Switching on the Lights

A cornerstone of SMLM is its use and control of the photo-activatable, photo-convertible, or photo-switchable (termed photo-modulatable in this article) properties of certain organic fluorophores/dyes and fluorescent proteins. This feature is so crucial to the functioning of the approach that it has become the principal reason behind the large suite of techniques surrounding SMLM such as PALM, FPALM, STORM, dSTORM, and PALMIRA. These techniques all share the same principle of stochastically switching-on fluorescent molecules to minimize their visual overlap in a sequence of images thus permitting the precise localization of individual molecules. The imaging hardware and analysis algorithms vary only slightly for each approach and are fairly simple to establish[15] (see Figure 2). Where the methods diverge is in the various classes of fluorophores used and the underlying protocol to either induce or control their photo-modulatable properties.

While PALM and FPALM have chosen genetically encoded fluorophores as their label of choice, STORM on the other hand, exploits the photo-switching properties of fluorescent dyes (such as Cy5 or Alexa647) when in close proximity to a secondary fluorescent dye label (such as Cy3) that functions as a fluorescence re-activator after bleaching. dSTORM[16] has further simplified the sample labeling (making it similar to that of classical immuno-fluorescence) by showing that similar photo-switching properties can be induced in several fluorescent dyes without the necessity of a secondary reactivator fluorescent dye label. This is accomplished by using a compatible high-intensity laser that sufficiently stimulates bleached fluorophores to return to a fluorescent state.

Both PALM, FPALM, STORM, and dSTORM experiments are typically divided into three distinct steps (see Figure 1). PALMIRA demonstrated that both the activation and readout steps can be taken simultaneously while independently acquiring a sequence of images.[8] Given the correct illumination conditions of both the activation and excitation light-sources, it is possible to obtain a time-lapse dataset, in which only a few fluorophores in a fluorescent on-state are captured per raw frame before they are immediately pushed into a non-detectable off-state. This procedure permits the acceleration of the acquisition by merging the two previously distinct activation and readout steps, and removes the need for the pulsing of the activation laser, which is incompatible with most acquisition software available.

Live cell SMLM is thus far almost only compatible with PALM or its sister techniques, which use genetically-encoded fluorophores. STORM and dSTORM use synthetic fluorescent dyes and special buffers able to maintain photo-switching. These buffers are, in general, highly toxic to cells. Later in this review we will examine emerging approaches that seek to overcome these limitations.

Switching on the Lights: Genetically Encoded Fluorophores

Perhaps the greatest advantage of genetically-encoded fluorescent proteins is the capacity to specifically label molecules in a non-invasive and live-cell compatible manner when compared to other methods such as immuno-fluorescence staining.

Furthermore, cell-friendly mediums can be applied as opposed to the photo-switching buffers commonly used in STORM and dSTORM.

Interestingly, it has been known for many years that GFP itself switches between a fluorescent state and a dark state in response to light.[17] However, it was the engineering of proteins to change their spectral properties upon illumination with light of specific wavelengths that allowed for the possibility of SMLM to become a widely used tool in cell biology. There are now numerous examples of these proteins, each with slightly different photo-physical characteristics. Photo-activatable proteins, such as PA-GFP, undergo a single transition from a non-fluorescent to a fluorescent state upon light-induced activation; reversible photo-switchable fluorophores are capable of multiple cycles of activation from a dark to a fluorescent state and return to a dark state, as in the case of Dronpa; photo-shiftable proteins, exemplified by mEos2, can be stimulated to convert between two spectrally distinct fluorescent forms (colors) by activating irradiation. These switching processes are manipulated by careful control of the imaging environment in tandem to the activation and excitation light intensities. This procedure permits for small subsets of fluorophores to be activated and rapidly bleach while captured in a sequence of images.

Most of the published literature on live-cell SMLM has utilized genetically-encoded fluorophores. Yet care needs to be taken when approaching these methods. Most photo-modulatable fluorophores require activation by near-UV light, which is toxic to the majority of cells. The Dendra2 fluorophore is a minor exception, since it can be activated at wavelengths close to a 488 nm wavelength (reviewed in Ref. 18). In most experiments it is also desirable that fluoro-phores immediately bleach following activation in order to eliminate their presence from multiple acquired images where they would augment the probability of particle spatial-overlap. A strong excitation light is then applied to bleach the fluorophores but the penalty is increased photo-toxicity.

For live-cell imaging in SMLM the "hardware" challenge can be partially overcome by using lower excitation intensities. This can be used to analyze the motility of the activated portion of fluorophores over a small sequence of images until the population is bleached, a process that can be repeated several times. If the fluorophores are confined to a specific cellular structure or location and motility is sufficiently slow so as not to cause blur artifacts (which degrade particle localization), then it becomes possible to reconstruct the domains where the fluorophores have been captured. This process uses each fluorophore multiple times to landmark their enclosing territory and causes less cell damage due to the reduction in the illumination intensity. Similarly, this strategy can also be used to study and map single-molecule motion as demonstrated by the single particle tracking PALM (sptPALM) technique that combines single-particle tracking with PALM microscopy[19] (see Figure 1).

The emergence of proteins with different emission spectra, such as rsCherry, a monomeric red photo-swichable fluorescent protein,[20] has made multi-color time-lapse SMLM imaging possible. Further, the development of new fluorescent proteins coupling photo-activatable and photo-shiftable properties, such as mIrisFP, introduces the possibility of using a pulse-chase approach in conjunction with super-resolution imaging for single particle tracking in dynamic processes, such as monomer turnover in macromolecules.[21]

Switching on the Lights: Synthetic Fluorophores

The two most important photophysical factors determining the spatial resolution are the brightness of the molecules in the fluorescent state used for localization, and the ratio between this state and the brightness of the molecules in the inactivated state. The former determines the number of photons that can be detected, which in turn determines the localization precision. The latter factor—the contrast ratio— contribute to the background, which again directly affects the localization precision. It should also be noted that the contrast ratio affects the resolution in a slightly more subtle way: low contrast ratios limit the ability of the system to localize molecules at high molecular densities, which is crucial for achieving high Nyquist-limited resolution.[14] Consequently, it is important to choose fluorescent labels that have both high brightness and high contrast ratios. Many of the most commonly used photo-modulatable fluorescent proteins have high contrast ratios but with a smaller photon output than many small-molecule fluorescent dyes (6000 photons per Cy5 molecule have been detected versus 490 photons per mEos molecule).[18] Therefore, small-molecule dyes may be attractive candidates as probes for live-cell SMLM. Yet, the impossibility of genetically encoding such labels leaves researchers with the difficult task of devising appropriate strategies for specific and sensitive targeting of fluorophores to biological molecules of interest, in a living cell. Cell membrane impermeability to many dyes and dye-conjugates, not least of all conventionally-labeled antibodies, stands as the greatest barrier to labeling intracellular targets under live-cell conditions, where the membrane should stay intact.

Currently available strategies fit into two broad categories—those that target fluorophores to peptide sequences or proteins fused to the target protein, and those that use enzymes to label the target sequence with the fluorescent tag (see Table I). The small labeling systems used by peptide-targeting labeling strategies, such as TetraCys,[22] HexaHis,[24] and PolyAsp,[23] cause minimal protein or cell perturbation. Thus far, however, only the TetraCys system has been successfully used in live-cell or intra-cellular labeling.[24] Protein-directed labeling, such as SNAP/CLIP tags,[26] Halo Tags,[27] and Dihydrofolate reductase (DHFR)

targeting with trimethoprim (TMP)-conjugates,[28,39] allows improved targeting specificity, but at the cost of an increase in the size of the recruiting system, increasing the risk of perturbing protein function. Despite this, the tag-dye conjugates in a number of these approaches are sufficiently cell permeable to allow intracellular labeling. Covalent labeling with the DHFR-based system has been successfully used in live-cell STORM imaging of Histone H2B dynamics.[39] Enzyme mediated protein labeling makes use of a small peptide sequence fused to the target protein and an enzyme, natural or engineered, which ligates the fluorescent probe to the recognition sequence. Some of these methods, such as those based on the use of sortase,[29,30] phosphopantetheine transferases,[33] and biotin ligase,[35] have been used to ligate fluorophore-conjugates to recognition sequences on target proteins in living cells or at the single molecule level. These approaches combine the benefits of a small directing peptide sequence and those of specific and rapid covalent labeling, and thus provide an ideal system for SMLM. However, the primary disadvantage currently encountered with the above systems is a lack of cell-permeability of the tags themselves, such that only membrane-protein labeling is possible.

In contrast, a Lipoic acid ligase-based system has been developed which makes labeling at both the cell membrane and intracellular targets possible.[36, 37] Two engineered forms of the microbial lipoic acid ligase have been developed by the Ting lab. The first is able to ligate cyclo-octyne conjugated probes to a Lipioic Acid Ligase Peptide (LAP) sequence fused to both cell surface and intracellular targets using a two-step process.[36–39] Practical challenges with the two-step process when applied to intracellular labeling led to the development of a second engineered ligase, a highly specific "fluorophoreligase," capable of specifically ligating hydroxycoumarin to intracellular LAP fusion proteins.[37] This newly engineered enzyme may be most suitable for the direct and specific labeling of intracellular targets, however, the strict restriction to only one dye limits the applicability of the system for SMLM at this stage. Further engineered forms, able to make use of multiple dye-conjugates, would provide a valuable system for multi-color labeling in live-cells in the future.

Besides strategies for the specific labeling of intracellular proteins with a wide variety of fluorescent dyes for live cell imaging, the suitability of specific fluorescent dyes for SMLM, particularly their photoswitching abilities, as well as the necessary conditions for such blinking, are also an important consideration, especially for live-cell imaging. Developments in imaging buffers have allowed photo-switching properties to be attributed to the majority of synthetic fluorescent dyes.

Switching on the Lights: Blinking-Inducing Buffers

Fluorescence excitation occurs by the absorption of a photon, which promotes a singlet, ground state molecule (S_0), to the excited singlet state (S_1). The subsequent return to S_0 produces a fluorescence photon emission. Alternatively the competing process of inter-system conversion can occur maintaining the fluorophore in a long-lived triplet state (T_1) formation (see Figure 3).

While in T_1 the fluorophore is unable to undergo fluorescence emission until relaxation to S_0 is re-achieved. During this period the fluorophore is sensitive to an irreversible photobleaching event if it reacts with molecular oxygen. This in turn results in the production of reactive oxygen species (ROS)—one of the major sources of photo-toxicity in cells. Notwithstanding, light-induced damage is not only created by this process but the overall absorption of light by the cell can produce toxicity.[38,40]

If reactions with oxygen can be avoided, then fluorophore photobleaching can be reversed. This process can be used to induce switching behavior in fluorophores[16,41] as the T_1 transition is stochastic and can be employed as the transient off-state of a fluorophore. Under these conditions, fluorophore blinking compatible with single molecule localization of a large population of fluorophores can be attained by imaging the cycling of short fluorophore photon bursts caused by S_0– S_1 transitions (the on-state) followed by the temporary arrest of fluorescence in the S_1–T_1 shift (the off-state). Initially, a very limited selection of dyes known to be able to undergo such photoswitching processes was available. Cyanine dyes[42,43] have been most commonly used for SMLM as they can be induced to switch by the presence of a second, activating fluorophore. Such a photoswitching mechanism requires oxygen removal and the use of millimolar concentrations of a reducing agent, such as β-mercaptoethanol, in the imaging medium.[42,44]

The demonstration of light-induced reversible photo-switching of single standard fluorophores for use in SMLM, termed dSTORM,[6] initiated significant advances in establishing SMLM imaging systems in which a much larger range of standard fluorophores can now be used. Central to these developments is an understanding of this "blinking" mechanism in fluorescent molecules, and concomitantly, the formulation of a system which modulates the switching rates (see Figure 3).

Photobleaching can be limited by the depletion of oxygen in the sample, either by embedding with poly-(vinyl-alcohol) (PVA) or using enzymatic oxygen scavenging buffers. This removes singlet oxygen and thus lengthens the T_1 lifetime, while addition of a reducing agent is often used to recover ionized fluorophores. The versatility of these approaches remains limited

by their dependence on the specific fluorophore's inherent single-state return rate for establishment of an appropriate rate of blinking, while oxygen depletion and toxic reducing agents make this setup incompatible with most live-cell experiments.

By approaching the photobleaching and triplet state recovery processes as a redox system, the Sauer and Tinnefeld groups have determined a simple, live-cell adaptable imaging setup to allow the fine-tuning of the rate of singlet-state return relative to triplet state formation. In this system, the reactive triplet state is rapidly depleted, either by oxidation to a radical cation, or by reduction to a radical anion. These ions can be recovered by the addition of a reducing or oxidizing agent, respectively, returning the fluorophore to the singlet state. Thus a buffering system with both reducing and oxidizing agents (termed ROXS) recovers reactive triplet state intermediates, repopulating the ground state and avoiding photobleaching.[45] By adjusting the relative ROXS buffer concentrations as required, the rate of photoswitching can be directly controlled to ensure sufficient fluorophores are in a dark state at each time point and that fluorescent lifetimes are sufficient to yield photons for accurate localization.[16,45]

The toxicity of ROXS reagents has had to be addressed in order to adapt the system for live-cell imaging (see Table II). Typically, thiol-reagents such as β-mercaptoethanol or β-mercaptoethylamine have been used as reducing agents in SMLM buffers.[16,41,44] Recently, glutathione and ascorbic acid have proven to be appropriate live-cell compatible alternatives to these reducing agents.[16,44,45] Despite its toxicity methylvialogen remains the primary oxidizing agent used.[45,48] By taking advantage of the oxidizing potential of oxygen itself, and using the molecular oxygen present in the cellular environment to fulfill the role of the oxidant in ROXS[16,48] the challenge of oxidant toxicity, as well as the need for oxygen-depletion in SMLM, has been neatly sidestepped. Although the presence of oxygen slightly restricts the experimentor's capacity to modulate the dyes' photophysics, this nevertheless greatly simplifies the application of ROXS for use in live-cell SMLM.

Essentially any desired fluorophore labeled with suitable photo-physical properties can be used in a biologically compatible ROXS imaging buffer, without the need for oxygen depletion. The ATTO dyes, such as ATTO520, ATTO565, ATTO655, ATTO680, and ATTO700, have proven particularly well suited for use in ''blink microscopy'' with ROXS.[16,48] Investigations are extending into the suitability of more water-soluble dyes, such as perylene dicarboximide fluorphores,[49] specifically for use in live-cell imaging.

ROXS provides a dye and buffer system that gives us prime choice of multi-color dyes to use in live-cell SMLM with minimal perturbation to the cell.

Breaking Through the Technological Limits

SMLM of a large population of fluorophores typically demands that hundreds to thousands of diffraction-limited images be acquired and processed in order to reconstruct a super-resolution dataset, the central ''software'' challenge. What is the relationship between localization precision and resolution? It is clear that the resolution of an SMLM image cannot be higher than the precision to which the molecules are localized. However, the Nyquist theorem, as applied here, requires that a structural-dynamics be sampled at twice the finest spatio-temporal resolution one βwants to detect. This is especially relevant in live-cell SMLM. In this case, a series of raw data frames are taken and subsequently parsed into SMLM time-points. For instance, if 1000 raw data frames are taken, one might parse these into 10 time-points of 100 raw data-frames or 100 time-points of 10 raw data frames. While the precision at which the molecules are localized does not change in either of these examples, the sparseness of detected particles will be far greater in the latter case than in the former case, and the underlying sample structure may be unrecognizable. Consequently, there is a fundamental trade-off between spatial and temporal resolution.

Additionally in order to obtain a reliable super-resolution reconstruction, algorithms have to analytically detect and localize each individual sub-diffraction particle present in each acquired frame. This is generally a major setback because visualization of the sample in parallel to the acquisition is crucial for making decisions on how to best adjust imaging conditions. Raw unprocessed images can be partially used to observe the sample but these are corrupted by the technique itself—each raw-image is generally composed of few emitting molecules not permitting a complete understanding of underlying cellular structures.

Recently several algorithms have been published allowing for processing speeds concurrent with the acquisition itself.[15,50–53] QuickPALM,[15] an ImageJ-based algorithm, in conjunction with IManager,[54] an open-source software for hardware control is able to both acquire and process 3D and 4D SMLM providing the super-resolution reconstruction in real-time as images are streamed from the camera (see Figure 2). This feature allows for data-driven algorithmic decisions on how to optimally adapt the acquisition and provides the user a reconstructed view of the sample being acquired.

A dominant challenge in SMLM is minimizing light-induced cell damage[55,56] as super-resolution techniques tend to dramatically increase the photo-damage caused to the cell by either increasing or prolonging the amount of light needed for imaging when compared to classical fluorescence microscopy. Conventionally in fluorescence imaging the entire field of view is illuminated uniformly, both light-excitation and acquisition time are adjusted so as to obtain a high enough signal-to-noise ratio (SNR) to resolve cellular structures of interest. Yet, fluorophore concentrations within cells vary, leaving researchers with the decision of how to best set the illumination characteristics at the cost of either under-exposing or over-exposing sub-regions of the image.

Controlled light-exposure microscopy (CLEM) introduces the concept of applying a non-uniform illumination to the imaging area in laser scanning systems where on a pixel-by-pixel basis the light-exposure is interrupted if a sufficient SNR has been achieved.[55] As a combination of "hardware" and "software" approaches, this method improves image-quality and severely reduces photo-toxicity.[55] Problematically, SMLM uses cameras that only permit the parallel acquisition of all the pixels composing an image theoretically preventing the implementation of CLEM. Non-uniform illumination in time has been previously applied to SMLM in the work of Betzig et al.[3] where the sample activation is incrementally increased over time to compensate for fluorophore depletion. This concept can be further adapted by modulating the illumination both in the spatial and temporal domain with the help of a spatial-light-modulator (SLM). In SMLM two light beams are used: a low-intensity activation beam to induce fluorophores into an on-state and a high-intensity readout beam to excite and bleach the fluorophore. By definition, the images acquired in SMLM have a sparse concentration of fluorophores. This means that most of the area subjected to illumination is not occupied by active fluorophores. By concentrating the readout illumination to the areas where only actively emitting fluoro-phores are present, a drastic reduction in the amount of light used for imaging is achieved therefore minimizing cell damage. A major focus of the QuickPALM[16] development team is to bring this feature forward by combining the power of real-time processing with the capacity for both SLM and acquisition hardware control brought by μManager.[54]

The authors thank members of the Mhlanga and Zimmer Lab for comments. They especially thank C. von Middendorff, C. Zimmer, and T. Duong for valuable comments and advice.

REFERENCES

1. Abbe, E. Arch Mikroskop Anat 1873, 9, 413–420.
2. Pertsinidis, A.; Zhang, Y.; Chu, S. Nature 2010, 466, 647–651.
3. Betzig, E.; Patterson, G. H.; Sougrat, R.; Lindwasser, O. W.; Olenych, S.; Bonifacino, J. S.; Davidson, M. W.; Lippincott-Schwartz, J.; Hess, H. F. Science 2006, 313, 1642–1645.
4. Hess, S. T.; Girirajan, T. P.; Mason, M. D. Biophys J 2006, 91, 4258–4272.
5. Rust, M.; Bates, M.; Zhuang, X. Nat Methods 2006, 3, 793–796.
6. Heilemann, M.; van de Linde, S.; Schuttpelz, M.; Kasper, R.; Seefeldt, B.; Mukherjee, A.; Tinnefeld, P.; Sauer, M. Angew Chem Int Ed Engl 2008, 47, 6172–6176.
7. Fölling, J.; Belov, V.; Kunetsky, R.; Medda, R.; Schönle, A.; Egner, A.; Eggeling, C.; Bossi, M.; Hell, S. Angew Chem Int Ed 2007, 46, 6266–6270.
8. Egner, A.; Geisler, C.; von Middendorff, C.; Bock, H.; Wenzel, D.; Medda, R.; Andresen, M.; Stiel, A.; Jakobs, S.; Eggeling, C. Biophys J 2007, 93, 3285.
9. Bock, H.; Geisler, C.; Wurm, C.; von Middendorff, C.; Jakobs, S.; Schönle, A.; Egner, A.; Hell, S.; Eggeling, C. Appl Phys B Lasers Opt 2007, 88, 161–165.
10. Carlton, P. M.; Boulanger, J.; Kervrann, C.; Sibarita, J. B.; Salamero, J.; Gordon-Messer, S.; Bressan, D.; Haber, J. E.; Haase, S.; Shao, L.; Winoto, L.; Matsuda, A.; Kner, P.; Uzawa, S.; Gustafsson, M.; Kam, Z.; Agard, D. A.; Sedat, J. W. Proc Natl Acad Sci USA 2010, 107, 16016–16022.
11. Burns, D. H.; Callis, J. B.; Christian, G. D.; Davidson, E. R. Appl Opt 1985, 24, 154–161.
12. Bobroff, N. Rev Sci Instrum 1986, 57, 1152–1157.
13. Hess, S.; Gould, T.; Gudheti, M.; Maas, S.; Mills, K.; Zimmerberg, J. Proc Natl Acad Sci USA 2006, 104, 17370–17375.
14. Shroff, H.; Galbraith, C. G.; Galbraith, J. A. Betzig, E. Nat Methods 2008, 5, 417–423.
15. Henriques, R.; Lelek, M.; Fornasiero, E. F.; Valtorta, F.; Zimmer, C.; Mhlanga, M. M. Nat Methods 2010, 7, 339–340.
16. van de Linde, S.; Endesfelder, U.; Mukherjee, A.; Schuttpelz, M.; Wiebusch, G.; Wolter, S.; Heilemann, M.; Sauer, M. Photochem Photobiol Sci 2009, 8, 465–469.
17. Dickson, R.; Cubitt, A.; Tsien, R. Moerner, W. Nature 1997, 388, 355–358.
18. Henriques, R.; Mhlanga, M. M. Biotechnol J 2009, 4, 846– 857.
19. Manley, S.; Gillette, J. M.; Patterson, G. H.; Shroff, H.; Hess, H. F.; Betzig, E.; Lippincott-Schwartz, J. Nat Methods 2008, 5, 155–157.
20. Subach, F. V.; Patterson, G. H.; Manley, S.; Gillette, J. M.; Lippincott-Schwartz, J.; Verkhusha, V. V. Nat Methods 2009, 6, 153–159.
21. Fuchs, J.; Bohme, S.; Oswald, F.; Hedde, P. N.; Krause, M.; Wiedenmann, J.; Nienhaus, G. U. Nat Methods 2010, 7, 627–630.
22. Adams, S. R.; Campbell, R. E.; Gross, L. A.; Martin, B. R.; Walkup, G. K.; Yao, Y.; Llopis, J.; Tsien, R. Y. J Am Chem Soc 2002, 124, 6063–6076.
23. Martin, B. R.; Giepmans, B. N.; Adams, S. R.; Tsien, R. Y. Nat Biotechnol 2005, 23, 1308–1314.
24. Guignet, E. G.; Segura, J. M.; Hovius, R.; Vogel, H. ChemPhys Chem 2007, 8, 1221–1227.
25. Ojida, A.; Honda, K.; Shinmi, D.; Kiyonaka, S.; Mori, Y.; Hamachi, I. J Am Chem Soc 2006, 128, 10452–10459.
26. Gautier, A.; Juillerat, A.; Heinis, C.; Corrêa I. R., Jr.; Kindermann, M.; Beaufils, F.; Johnsson, K. Chem Biol 2008, 15, 128–136.
27. Los, G. V.; Encell, L. P.; McDougall, M. G.; Hartzell, D. D.; Karassina, N.; Zimprich, C.; Wood, M. G.; Learish, R.; Ohana, R. F.; Urh, M.; Simpson, D.; Mendez, J.; Zimmerman, K.; Otto, P.; Vidugiris, G.; Zhu, J.; Darzins, A.; Klaubert, D. H.; Bulleit, R. F.; Wood, K. V. ACS Chem Biol 2008, 3, 373–382.
28. Miller, L. W.; Cai, Y.; Sheetz, M. P.; Cornish, V. W. Nat Methods 2005, 2, 255–257.
29. Popp, M. W.; Antos, J. M.; Grotenbreg, G. M.; Spooner, E.; Ploegh, H. L. Nat Chem Biol 2007, 3, 707–708.
30. Yamamoto, T.; Nagamune, T. Chem Commun (Camb) 2009, 1022–1024.
31. Lin, C. W.; Ting, A. Y. J Am Chem Soc 2006, 128, 4542–4543.
32. Sunbul, M.; Yin, J. Org Biomol Chem 2009, 7, 3361.

33. Zhou, Z.; Cironi, P.; Lin, A. J.; Xu, Y.; Hrvatin, S.; Golan, D. E.; Silver P. A.; Walsh, C. T.; Yin, J. ACS Chem Biol 2007, 2, 337–346.
34. Jacquier, V.; Prummer, M.; Segura, J. M.; Pick, H.; Vogel, H. Proc Natl Acad Sci USA 2006, 103, 14325–14330.
35. Howarth, M.; Chinnapen, D. J.; Gerrow, K.; Dorrestein, P. C.; Grandy, M. R.; Kelleher, N. L.; El-Husseini, A.; Ting, A. Y. Nat Methods 2006, 3, 267–273.
36. Fernandez-Suarez, M.; Baruah, H.; Martinez-Hernandez, L.; Xie, K. T.; Baskin, J. M.; Bertozzi, C. R.; Ting, A. Y. Nat Biotech-nol 2007, 25, 1483–1487.
37. Uttamapinant, C.; White, K. A.; Baruah, H.; Thompson, S.; Fernandez-Suarez, M.; Puthenveetil, S.; Ting, A. Y. Proc Natl Acad Sci USA 2010, 107, 10914–10919.
38. Baruah, H.; Puthenveetil, S.; Choi, Y. A.; Shah, S.; Ting, A. Y. Angew Chem Int Ed Engl 2008, 47, 7018–7021.
39. Wombacher, R.; Heidbreder, M.; van de Linde, S.; Sheetz, M. P.; Heilemann, M.; Cornish, V. W.; Sauer, M. Nat Methods 2010, 7, 717–719.
40. Stephens, D. J.; Allan, V. J. Science 2003, 300, 82–86.
41. Fo¨lling, J.; Bossi, M.; Bock, H.; Medda, R.; Wurm, C. A.; Hein, B.; Jakobs, S.; Eggeling, C.; Hell, S. W. Nat Methods 2008, 5, 943–945.
42. Bates, M.; Huang, B.; Dempsey, G. T.; Zhuang, X. Science 2007, 317, 1749–1753.
43. Bates, M.; Blosser, T. R.; Zhuang, X. Phys Rev Lett 2005, 94, 108101.
44. van de Linde, S.; Kasper, R.; Heilemann, M.; Sauer, M. Appl Phys B Lasers Opt 2008, 93, 725–731.
45. Vogelsang, J.; Kasper, R.; Steinhauer, C.; Person, B.; Heilemann, M.; Sauer, M.; Tinnefeld, P. Angew Chem Int Ed 2008, 47, 5465–5469.
46. Rasnik, I.; McKinney, S. A.; Ha, T. Nat Methods 2006, 3, 891–893.
47. Aitken, C. E.; Marshall, R. A.; Puglisi, J. D. Biophys J 2008, 94, 1826–1835.
48. Vogelsang, J.; Cordes, T.; Forthmann, C.; Steinhauer, C.; Tinnefeld, P. Proc Natl Acad Sci USA 2009, 106, 8107–8112.
49. Cordes, T.; Vogelsang, J.; Anaya, M.; Spagnuolo, C.; Gietl, A.; Summerer, W.; Herrmann, A.; Mullen, K.; Tinnefeld, P. J Am Chem Soc 2010, 132, 2404–2409.
50. Wolter, S.; Schuttpelz, M.; Tscherepanow, M.; van de Linde, S.; Heilemann, M.; Sauer, M. J Microsc 2010, 237, 12–22.
51. Hedde, P. N.; Fuchs, J.; Oswald, F.; Wiedenmann, J.; Nienhaus, G. U. Nat Methods 2009, 6, 689–690.
52. Smith, C. S.; Joseph, N.; Rieger, B.; Lidke, K. A. Nat Methods 2010, 7, 373–375.
53. Quan, T.; Li, P.; Long, F.; Zeng, S.; Luo, Q.; Hedde, P. N.; Nienhaus, G. U.; Huang, Z. L. Opt Express 2010, 18, 11867–11876.
54. Stuurman, N.; Amodaj, N.; Vale, R.D. Microsc Today 2007, 15, 42–43.
55. Hoebe, R. A.; Van Oven, C. H.; Gadella, T. W., Jr.; Dhonukshe, P. B.; Van Noorden, C. J.; Manders, E. M. Nat Biotechnol 2007, 25, 249–253.
56. Hoebe, R. A.; Van der Voort, H. T.; Stap, J.; Van Noorden, C. J.; Manders, E. M. J Microsc 2008, 231, 9–20.

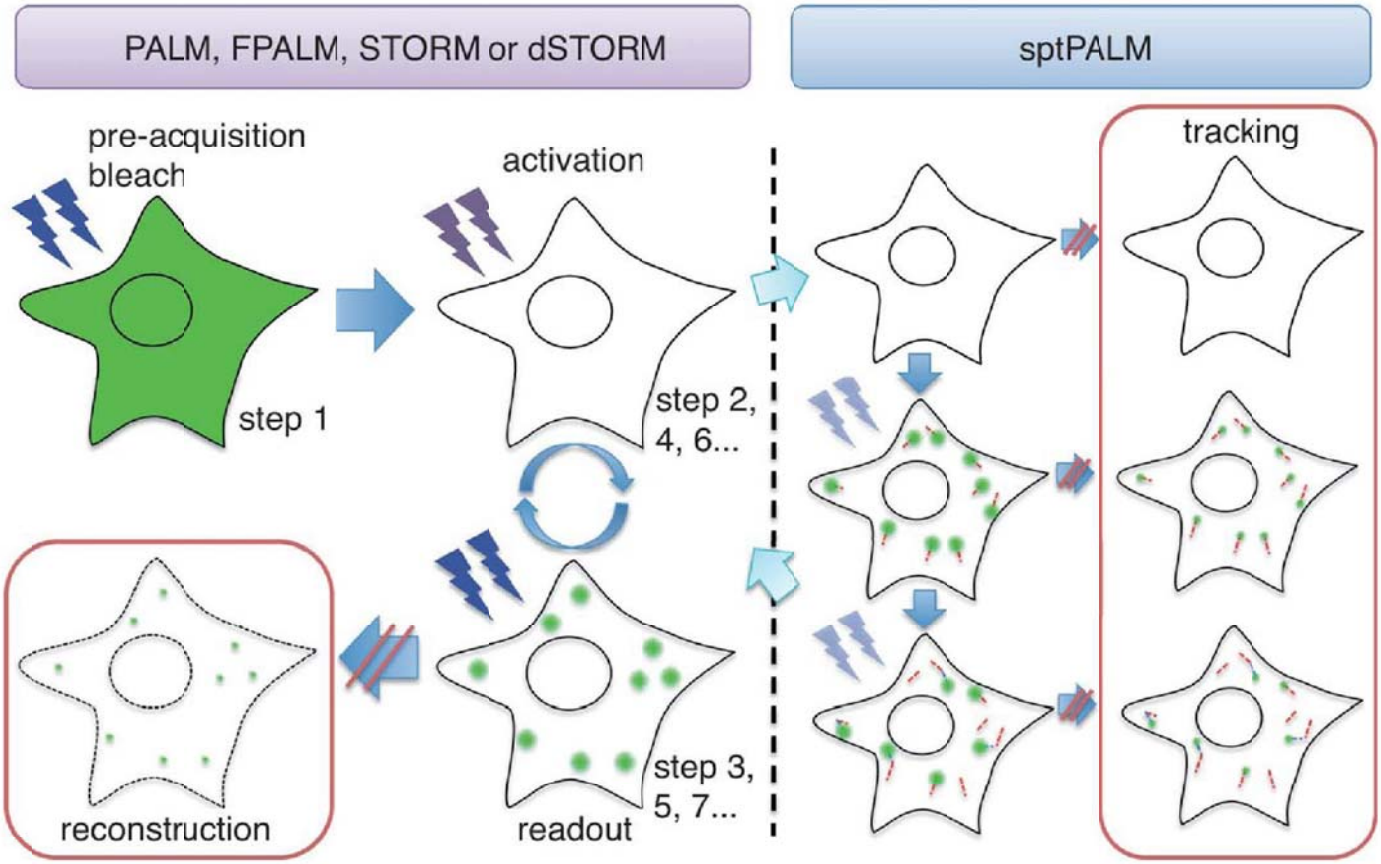

FIGURE 1 Acquisition steps for PALM, FPALM, STORM, dSTORM, and sptPALM. The typical acquisition in SMLM for PALM, FPALM, STORM, and dSTORM is divided in three independent steps: pre-activation bleach—where cells are illuminated by a strong excitation laser, forcing any unwanted active fluorophore to go into an off-state; activation—the light-induced activation of an extremely reduced number of fluorophores preventing excessive spatial-overlapping of the visualized particles; readout—excitation and imaging of the activated fluorophores followed by bleaching to minimize the presence of already visualized particles in posterior acquired images. These final two-steps can be cycled until a sufficient number of molecules have been identified. In parallel to the readout phase particles can be detected and assembled into a reconstruction. On sptPALM, the readout phase is divided into multiple images where particle movement is captioned and tracked in parallel until bleaching of most active fluorophores has occurred leading to a new imaging cycle started by the activation phase.

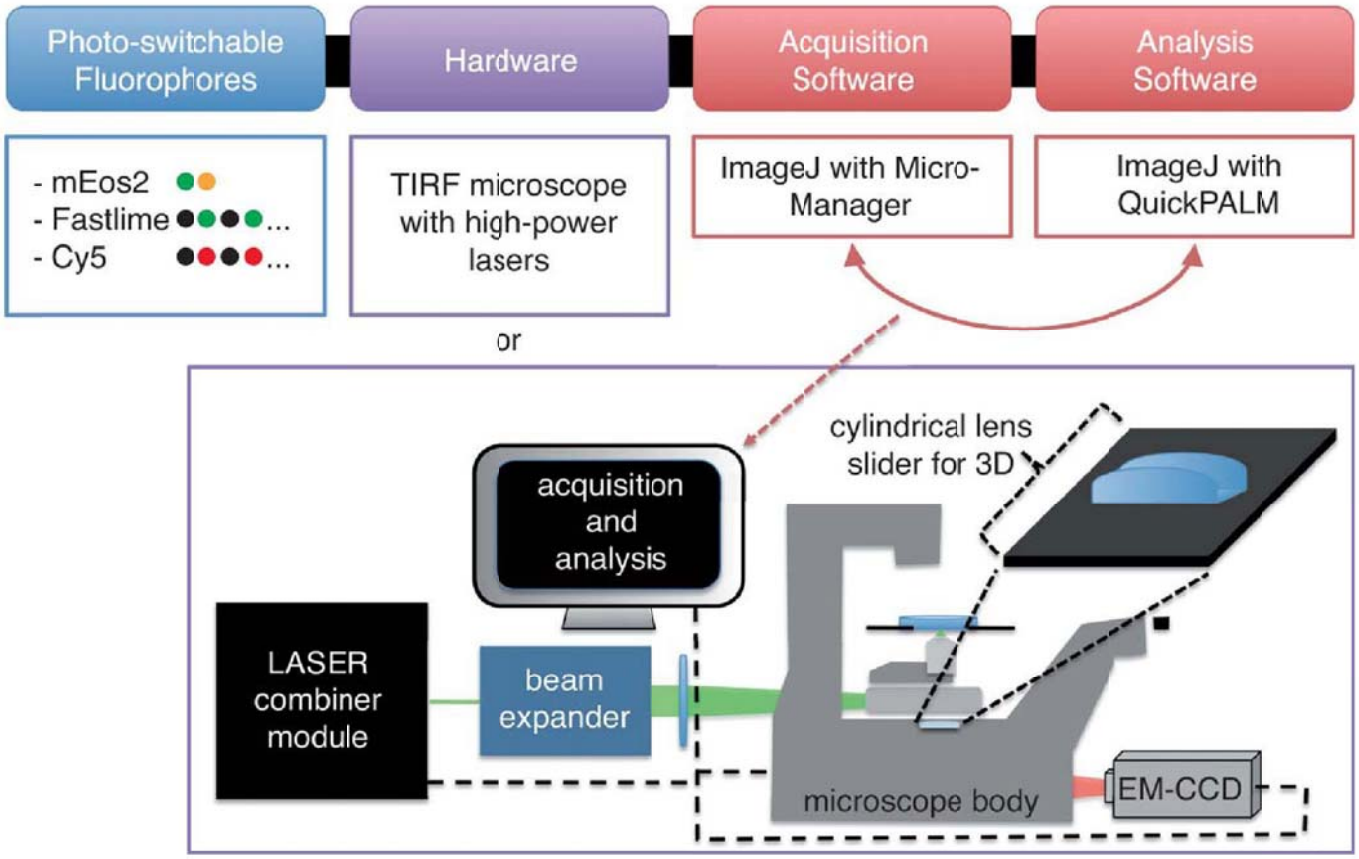

FIGURE 2 Setting your own SMLM. Aside from the complexities involving fluorophore selection discussed extensively in this review, assembling a SMLM compatible microscope is both cost-effective and straightforward. TIRF microscopes can easily be adapted for SMLM or a custom system can be set up by combining a commercial microscope body with a high-sensitivity camera and a custom laser excitation system. A cylindrical lens inserted into a slider below the objective revolver can provide astigmatism characteristics enabling 3D imaging with the system—an extensive list of tutorials on the subject can be found in http://code.google.com/p/quickpalm. Manager constitutes a free, open-source software for hardware control and acquisition compatible with SMLM experiments and can be used in tandem with QuickPALM—a dedicated ImageJ plugin to process SMLM data.

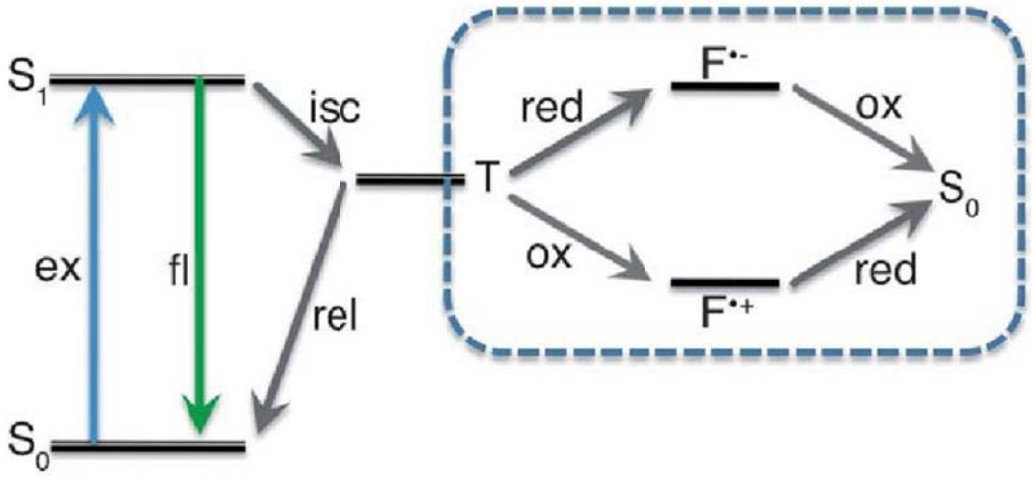

FIGURE 3 Scheme of the photoswitching process and redox triplet state depletion mechanism. A ground state fluorophore is excited to the S1 singlet state by the absorbtion of a photon. The fluorophore may then return to the ground state or transverse into a dark triplet state by intersystem crossing, followed by stochastic relaxation back to ground state. Boxed region: The addition of reducing and oxidizing agents depletes the triplet state by electron transfer reactions, producing either form of fluorophore radical and retrieving the reactive intermediates by the reciprocal reduction or oxidation. This returns the fluorophore to ground state, avoiding photobleaching and allowing cycling or switching of the fluorophore between excited, triplet, and ground states. S0: ground state; S1: excited singlet state; T: triplet state; ex: excitation; fl: fluorescence; isc: inter-systen crossing; rel: relaxation; red: reduction; ox: oxidation; F: fluorophore.

Table I Targeting Strategies for Synthetic Dyes

Targeting Peptide	Ligand	Enzyme	Bond	Cellular Targets	Comments	Reference
Peptide/protein-based targeting						
TetraCys	Biarsenical fluorophores	—	Covalent	Membrane/intracellular proteins	Live imaging with FlAsH tags	22,23
HexaHis	NTA-conjugates	—	Noncovalent	Membrane proteins	N/A	24
PolyAsp	Dpa tyr conjugates	—	Noncovalent	Membrane proteins	N/A	25
SNAP/CLIP tags	Benzylguanine conjugates	AGT	Covalent	Membrane/intracellular proteins	Greater specificity, larger label	26
Halo tags	Chlorcalkane conjugates	Dehalogenase	Covalent	Membrane/intracellular proteins	Greater specificity, larger label	27
DHFR	TMP	DHFR	Noncovalent or covalent	Membrane/intracellular proteins	Greater specificity, larger label	25,28
Enzyme-based targeting						
Sortag	Oligo-glycine dye conjugate	Sortase	Covalent	Membrane proteins, C- and N-terminals	N/A	29,30
Q-tag	Amine-modified probes	Transglutaminase	Covalent	Membrane proteins, N-terminal	Low substrate specificity	31,32
ACP/PCP	Co-enzyme A-conjugates	Phosphopantetheine transferases (Sfp and AcpS)	Covalent	Membrane proteins	N/A	33,34
AP	Biotin conjugates	Biotin ligase, BirA	Covalent	Membrane proteins	N/A	35
LAP	cyclo-octyne conjugates/ hydroxycoumarin	Lipoic acid ligase	Covalent	Membrane/intracellular proteins	One or two-step process	36–38

DHFR: dihydrofolate reductase; ACP: acyl-carrier protein; PCP: peptidyl-carrier protein; AP: biotin ligase acceptor peptide; LAP: lipoic acid ligase acceptor peptide; NTA: nitrilotriacetic acid; TMP: trimethoprim; AGT: O^6-alkylguanine-DNA alkyltransferase; N/A: not applicable

Table II Redox Buffer Agents to Modulate Photo-Switching

Redox Buffer	Action	Endogenous	Toxicity	Reference
Trolox	Reductant	No	Low	46
b-mercaptoethanol	Reductant	No	High	44,46,47
Propyl galate	Reductant	No	Low	46
Ascorbic acid	Reductant	Yes	Low	46,48
Glutathione	Reductant	Yes	Low	44,46,48
Dithiotriotol	Reductant	No	High	47
Tris(2-carboxyethyl)phosphine hydrochloride	Reductant	No	High	47
Methylviologen	Oxidant	No	High	16,45,48
Ambient oxygen	Oxidant	Yes	Low	16,48